

Ti₂Nb₆O₁₂, a Novel Niobium Oxide Cluster Compound with “Chevrel Phase” Intercluster Connectivity Type

Ekaterina V. Anokhina, Michael W. Essig, Cynthia S. Day, and Abdessadek Lachgar*

Contribution from the Department of Chemistry, Wake Forest University,
Winston-Salem, North Carolina 27109

Received March 8, 1999

Abstract: The niobium oxide cluster compound Ti₂Nb₆O₁₂ was synthesized from NbO, NbO₂, and TiO₂ in the presence of NaF melt at 950 °C. It crystallizes in an original structure type based on octahedral cluster units (Nb₆O₁₂)O₆^a. The clusters connect to each other through outer–inner linkages to form a three-dimensional framework containing cubeoctahedral cavities. The cluster connectivity pattern in Ti₂Nb₆O₁₂ and intercluster metal–metal distances are similar to those found in the “Chevrel phases”. The Ti⁴⁺ ions have a distorted octahedral environment formed by the oxide ligands belonging to the clusters. Band structure calculations indicate that the lowest unoccupied band in Ti₂Nb₆O₁₂ resembles the conduction band in the superconducting “Chevrel phases”.

Introduction

The formation of metal–metal bonds is a characteristic feature of compounds containing early transition metals in low oxidation states.^{1,2} In these metal-rich compounds, discrete or condensed octahedral metal clusters are commonly encountered.³ The M₆ octahedron can be surrounded by ligands in two ways, giving M₆L₁₄ or M₆L₁₈ cluster units. In M₆L₁₄-type clusters, typical for molybdenum and rhenium halides, chalcogenides, and chalcogenides,⁴ eight “inner” ligands (Lⁱ) cap the octahedron faces and six “outer” ligands (L^a) are located in the apical positions.⁵ For metals with a smaller number of valence electrons, the M₆L₁₈-type clusters in which 12 “inner” ligands bridge the edges of the M₆ octahedron and 6 “outer” ligands occupy apical positions predominate. These units are found in reduced zirconium, niobium, tantalum, and rare earth halides,⁶ molybdenum and tungsten oxides,^{7,8} and niobium and tantalum oxides^{9,10} and oxochlorides.^{11,12} The clusters can connect to each other through inner and/or outer ligands, or by direct condensation of the metal octahedra, to form a variety of frameworks with different degrees of metal–metal bonding.

“Chevrel phases”, which are molybdenum chalcogenides with the general formula A_xMo₆L₈ (A = Pb, Sn, Cu, Li, La, Eu,

etc.; L = S, Se, Te),^{13,14} constitute one of the most remarkable series of cluster compounds due to their unusual physical properties. They exhibit superconductivity at high critical magnetic fields, and simultaneous existence of magnetic order and superconductivity.¹⁵ Their three-dimensional frameworks are based on Mo₆L₁₄ cluster units connected through “outer–inner” linkages (L^{a-i}) to give the connectivity pattern (Mo₆S_{6/2}^{i-a}S₂)_{6/2}^{a-i}. This type of linkage leads to short intercluster Mo–Mo distances (3.1–3.6 Å) that allow for weak metal–metal intercluster interactions. Extensive investigations of the “Chevrel phases” show that their structural and physical properties can be tuned by changing the nature and concentration of the metal atoms A, ligand substitution,¹⁴ and molybdenum substitution by other transition metals.^{16–18} The “outer–inner” type linkages also exist in compounds containing M₆L₁₈-type clusters;^{19–26} however, in contrast to the “Chevrel phases”, the intercluster metal–metal separation is large (4.0–4.9 Å) due to ligand steric effects.²⁷

The motivation for our research program in this area is the preparation and characterization of materials with short inter-

- (1) Simon, A. *Angew. Chem., Int. Ed. Engl.* **1988**, *27*, 159–183.
- (2) Hughbanks, T. *J. Alloys Compd.* **1995**, *229*, 40–53.
- (3) Perrin, C. *J. Alloys Compd.* **1997**, *262–263*, 10–21.
- (4) Perrin, A.; Perrin, C.; Sergent, M. *J. Less-Common Metals* **1988**, *137*, 241–265.
- (5) Schäfer, H.; von Schnering, H. G. *Angew. Chem.* **1964**, *76*, 833–849.
- (6) Corbett, J. D. In *Modern Perspectives in Inorganic Crystal Chemistry*; Parthé, E., Ed.; Kluwer Academic Publishers: The Netherlands, 1992.
- (7) Hibble, S. J.; Cooper, S. P.; Hannon, A. C.; Patat, S.; McCarroll, W. H. *Inorg. Chem.* **1998**, *37*, 6839–6846.
- (8) McCarley, R. E. In *Early Transition Metal Clusters with π-Donor Ligands*; Chisholm, M. H., Ed.; VCH Publishers: New York, 1995.
- (9) Köhler, J.; Svensson, G.; Simon, A. *Angew. Chem., Int. Ed. Engl.* **1992**, *31*, 1437–1456.
- (10) Ritter, A.; Lydssan, T.; Harbrecht, B. Z. *Allg. Anorg. Chem.* **1998**, *684*, 1791–1795.
- (11) Anokhina, E. V.; Essig, M. W.; Lachgar, A. *Angew. Chem., Int. Ed. Engl.* **1998**, *37*, 522–525.
- (12) Ogliaro, F.; Cordier, S.; Halet, J.-F.; Perrin, C.; Sailard, J.-Y.; Sergent, M. *Inorg. Chem.* **1998**, *37*, 6199–6207.

- (13) Chevrel, R.; Sergent, M.; Prigent, J. *J. Solid State Chem.* **1971**, *3*, 515–519.
- (14) Fischer, Ø.; Maple, M. B., Eds. *Superconductivity in Ternary Compounds*; Top. Curr. Phys. 32; Springer-Verlag: Berlin, 1982.
- (15) Fischer, Ø. *Appl. Phys.* **1978**, *16*, 1–28.
- (16) Perrin, A.; Sergent, M.; Fischer, Ø. *Mater. Res. Bull.* **1978**, *13*, 259–264.
- (17) Perrin, A.; Chevrel, R.; Sergent, M.; Fischer, Ø. *J. Solid State Chem.* **1980**, *33*, 43–47.
- (18) Neuhausen, J.; Finckh, E. W.; Tremel, W. *Inorg. Chem.* **1996**, *35*, 5622–5626.
- (19) Smith, J. D.; Corbett, J. D. *J. Am. Chem. Soc.* **1985**, *107*, 5704–5711.
- (20) Hwu, S.-J.; Corbett, J. D. *J. Solid State Chem.* **1986**, *64*, 331–346.
- (21) Dudis, D. S.; Corbett, J. D.; Hwu, S.-J. *Inorg. Chem.* **1986**, *25*, 3434–3438.
- (22) Payne, M. W.; Corbett, J. D. *Inorg. Chem.* **1990**, *29*, 2246–2251.
- (23) Hughbanks, T.; Corbett, J. D. *Inorg. Chem.* **1988**, *27*, 2022–2226.
- (24) Artelt, H. M.; Schleid, T.; Meyer, G. Z. *Allg. Anorg. Chem.* **1992**, *618*, 18–25.
- (25) Artelt, H. M.; Meyer, G. Z. *Allg. Anorg. Chem.* **1993**, *619*, 1–6.
- (26) Uma, S.; Corbett, J. D. *Inorg. Chem.* **1998**, *37*, 1944–1948.
- (27) Corbett, J. D. *J. Solid State Chem.* **1981**, *37*, 335–357.

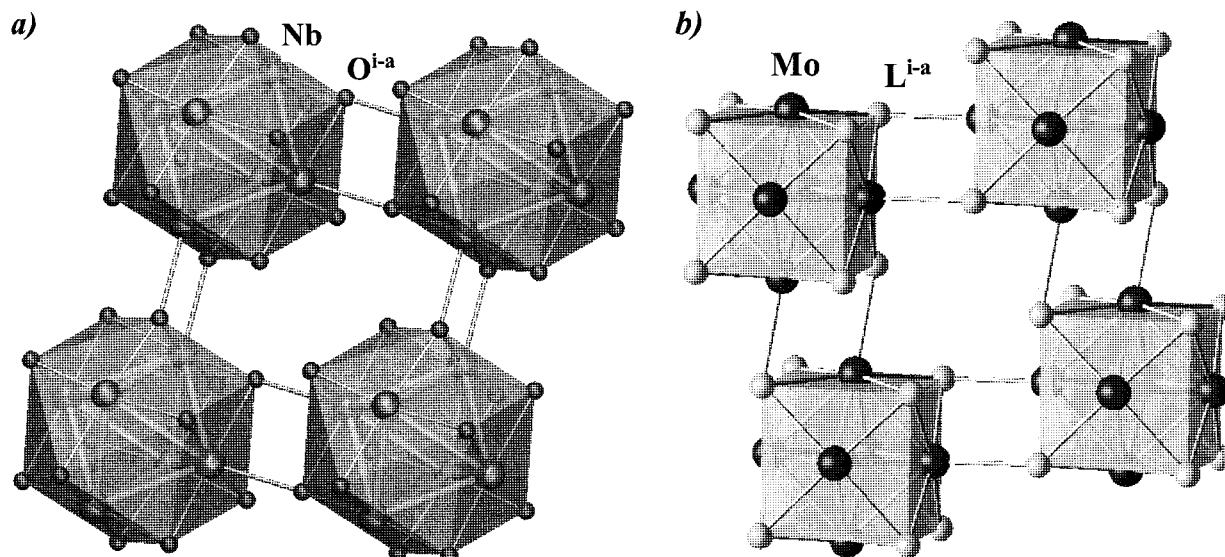


Figure 1. Cluster framework in $\text{Ti}_2\text{Nb}_6\text{O}_{12}$ generated by “inner–outer” linkages of Nb_6O_{18} clusters (a) and cluster framework in “Chevrel phases” generated by “inner–outer” linkages of Mo_6S_{14} clusters (b).

Table 1. Crystal Data and Structure Refinement for $\text{Ti}_2\text{Nb}_6\text{O}_{12}$

empirical formula	$\text{Ti}_2\text{Nb}_6\text{O}_{12}$
formula wt	$845.26 \text{ g}\cdot\text{mol}^{-1}$
crystal size	$0.1 \times 0.1 \times 0.1 \text{ mm}^3$
wavelength	Mo $K\alpha$ (0.71073 Å)
crystal system	trigonal
space group	$R\bar{3}$ (No. 148), hexagonal setting
unit cell dimensions	$a = 7.9364(5) \text{ Å}$, $c = 14.4339(10) \text{ Å}$
volume	$787.34(9) \text{ Å}^3$
Z	3
density (calcd)	$5.348 \text{ g}\cdot\text{cm}^{-3}$
absorption coeff	7.807 mm^{-1}
absorption corr	empirical, $T_{\text{min}} = 0.86$; $T_{\text{max}} = 0.99$
no. of reflns collected	795
no. of independent reflcs	562 ($R_{\text{int}} = 0.0138$)
no. of data/restraints/ parameters	562/0/33
goodness-of-fit on F^2	1.116
final R indices ($I > 2\sigma(I)$)	$R_1 = 0.0180$, $wR_2 = 0.0342$
R indices (all data)	$R_1 = 0.0219$, $wR_2 = 0.0349$

cluster separation. Reduced niobium oxides are suitable target systems due to the small ligand size and the variety of cluster connectivity previously found in these systems. Here, we report the synthesis, crystal structure, physical characterization, and band structure of the compound $\text{Ti}_2\text{Nb}_6\text{O}_{12}$, which crystallizes in an original structure type based on Nb_6O_{18} clusters and exhibits intercluster connectivity similar to that found in the “Chevrel phases” (Figure 1). The effect of the basic cluster type and cluster connectivity on the band structure of these materials is discussed.

Experimental Section

Synthesis. (a) Single Crystal Preparation. The title compound was initially obtained as black octahedral crystals from a reaction aimed at the synthesis of $\text{LiTi}_2\text{Nb}_6\text{Cl}_{14}\text{O}_4$. A stoichiometric mixture of Nb powder, NbCl_5 , Nb_2O_5 , Ti foil, and LiCl, handled in a dry atmosphere, was sealed under vacuum, in a quartz tube. The tube was heated in a tubular furnace at 950°C for 96 h, followed by cooling to 500°C in 96 h. The composition of the octahedral crystals was determined by energy-dispersive X-ray analysis (EDAX) with use of a Philips 515 scanning electron microscope equipped with a microprobe capable of detecting elements as light as carbon. The analysis indicated the presence of niobium, titanium, and oxygen in a 3:1:6 ratio.

(b) Quantitative Preparation. After the composition of the new phase was established by the crystal structure analysis, the compound

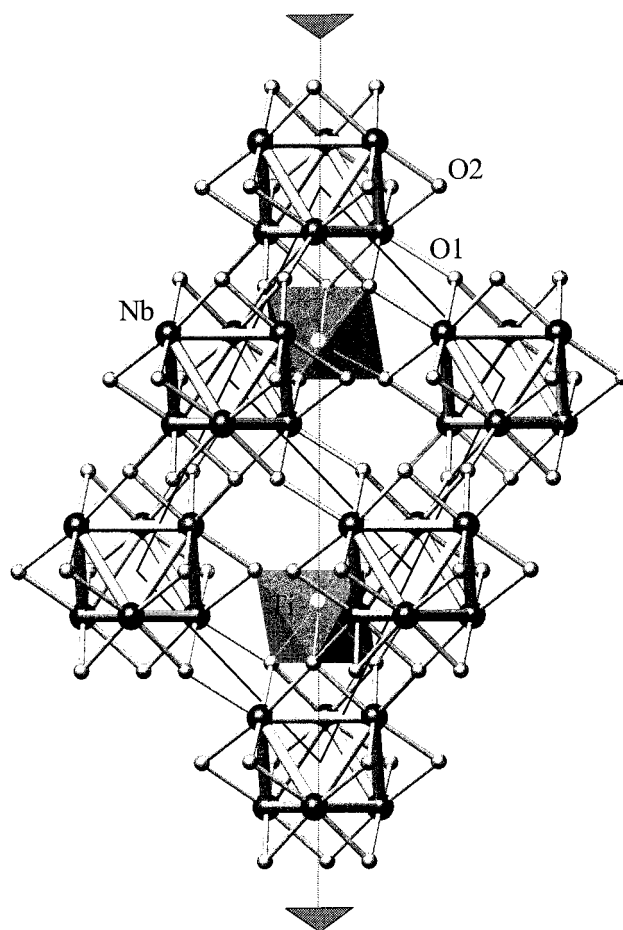


Figure 2. A projection of a primitive unit cell of $\text{Ti}_2\text{Nb}_6\text{O}_{12}$ perpendicular to the 3-fold axis.

$\text{Ti}_2\text{Nb}_6\text{O}_{12}$ was synthesized in high yield (>98%) from a stoichiometric mixture of NbO, NbO_2 , and TiO_2 in the presence of NaF melt (20% by mass). The powders were mixed thoroughly, pressed into a pellet, placed in an alumina boat, and sealed under vacuum in a quartz tube to protect the mixture from oxidation. The mixture was heated at 950°C for 96 h, then cooled to room temperature in 4 h. Extensive reaction of the NaF melt with the alumina and quartz containers was observed, which resulted in the presence of silicon, aluminum, and sodium in the raw product (as determined by EDAX analysis). The product was

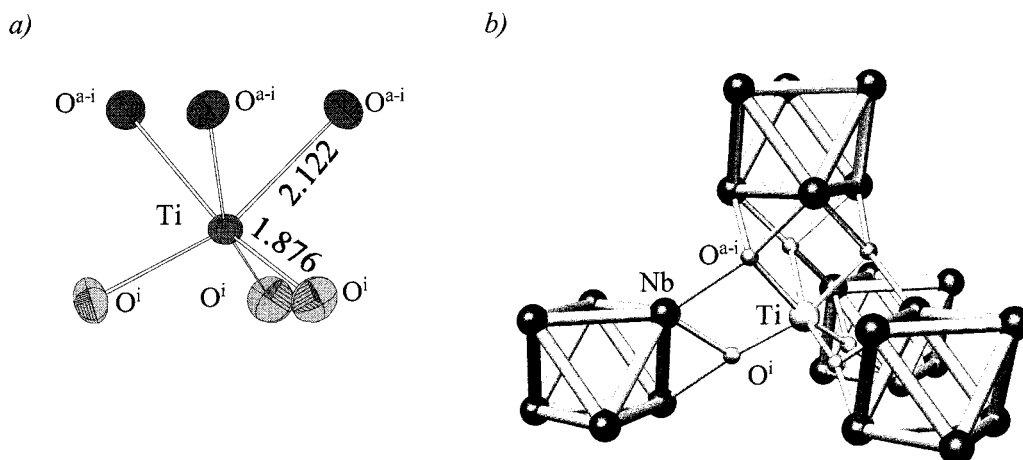


Figure 3. Titanium environment in Ti₂Nb₆O₁₂ (90% probability thermal ellipsoid view) (a) and linkages between the titanium ions and niobium clusters (b).

Table 2. Atomic Coordinates and Equivalent Isotropic Displacement Parameters (Å²) for Ti₂Nb₆O₁₂

	<i>x</i>	<i>y</i>	<i>z</i>	<i>U</i> _{eq} ^a
Nb	0.2174(1)	0.0218(1)	0.0780(1)	0.004(1)
Ti	0.6667	0.3333	0.0593(1)	0.004(1)
O1	0.0275(3)	-0.1796(3)	0.1733(1)	0.005(1)
O2	0.7429(3)	0.1723(3)	-0.0006(1)	0.007(1)

^a *U*_{eq} is defined as one-third of the trace of the orthogonalized *U*_{ij} tensor.

Table 3. Selected Bond Lengths (Å) and Angles (deg) for Ti₂Nb₆O₁₂

(Nb ₆ O ₁₈) Cluster Unit			
Nb–Nb			
Nb–Nb _(Δ)	2.8502(4) 2×	Nb–Nb'–Nb''	61.441(12)
Nb–Nb _(Δ-Δ)	2.7896(4) 2×	Nb–Nb'–Nb'''	59.279(6)
		Nb''–Nb–Nb'	60
Nb–O ^a			
Nb–O(1)	2.212(2)	Nb–O(1)–Nb'	161.85(10)
		Nb–O(1)–Nb''	99.17(8)
Nb–O ⁱ			
Nb–O(1)	2.076(2)	Nb–O(1)–Nb'	85.02(7)
Nb–O(1)'	2.142(2)	Nb–O(2)–Nb'	84.11(7)
Nb–O(2)	2.051(2)		
Nb–O(2)'	2.113(2)		
Titanium Environment			
Ti–O(2)	1.876(2) 3×	O(2)–Ti–O(2)'	100.47(8)
Ti–O(1)	2.122(2) 3×	O(2)'–Ti–O(1)	83.60(8)
		O(2)–Ti–O(1)'	96.23(8)
		O(1)–Ti–O(1)'	78.24(8)
Other Important Distances			
Nb–Ti			3.1758(3)
Nb–Ti'			3.2731(7)
Nb–Nb (intercluster)			3.3154(5)

subsequently washed with concentrated HF, 3 M KOH, and distilled water to remove these impurities. X-ray powder diffraction analysis showed the final product to consist of about 98% Ti₂Nb₆O₁₂ and 2% NbO. A combination of Energy and Wave Dispersive X-ray analyses of the final product confirmed the presence of titanium, niobium, and oxygen in a 1:3:6 ratio, the absence of fluorine, and the presence of NbO as an impurity (estimated at 2%).

Crystal Structure Determination. The crystal structure of Ti₂Nb₆O₁₂ was determined by using single-crystal X-ray diffraction. Three-dimensional intensity data were collected on an octahedral crystal with dimensions of about 0.1 × 0.1 × 0.1 mm³ with a Siemens P4 X-ray diffractometer. The unit cell parameters were refined based on 47 centered reflections to give a rhombohedral unit cell with *a* = 7.9364(5) Å and *c* = 14.4339(10) Å (hexagonal setting). The intensity data

Table 4. Parameters Used in Extended Hückel Calculations

	orbital	<i>H</i> _{ii} , eV	ζ ₁	ζ ₂	<i>C</i> ₁	<i>C</i> ₂
Ti ^a	3d	-10.81	4.55	1.40	0.42061	0.78391
	4s	-8.97	1.08			
	4p	-5.44	0.68			
Nb ^b	4d	-9.55	2.955	1.333	0.68585	0.46190
	5s	-8.27	1.428			
	5p	-5.31	1.035			
O ^a	2s	-32.3	2.28			
	2p	-14.8	2.28			

^a EHMACC built-in parameters. ^b Kennedy, J. R.; Adler, P.; Dronskowski, R.; Simon, A. *Inorg. Chem.* **1996**, *35*, 2276–82.

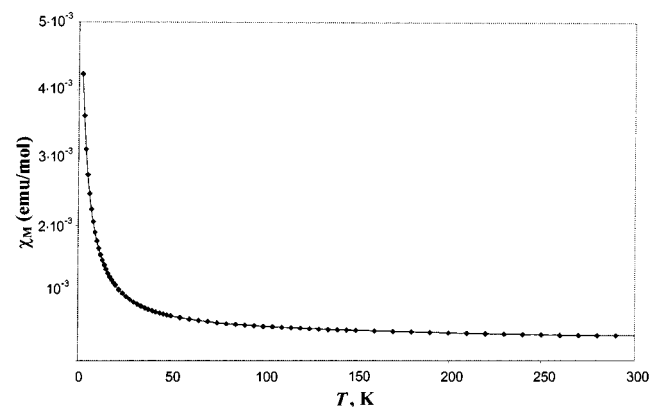


Figure 4. Molar magnetic susceptibility χ_M (emu/mol) of Ti₂Nb₆O₁₂ over the temperature range 300–2 K.

were corrected for Lorentz and polarization effects, and an empirical absorption correction based on ψ scans was applied. Extinction conditions suggested *R* $\bar{3}$ and *R*3 as possible space groups. The crystal structure was solved in the centrosymmetric space group *R* $\bar{3}$ using direct methods, and refinement of all atoms with anisotropic thermal parameters was carried out with use of the full-matrix least-squares techniques against *F*² (Shelxtl).²⁸ Subsequent refinement in the acentric space group *R*3 did not lead to statistically significant changes in reliability factors or GOF. Details of data collection and structure refinement are summarized in Table 1. Atomic positions and important bond distances and angles are shown in Tables 2 and 3, respectively.

Band Structure Calculations. The band structure calculations were carried out on the primitive unit cell using the extended Hückel tight-binding method.^{29–31} The atomic parameters used in the calculations are given in Table 4. The density of states and overlap populations

(28) Sheldrick, G. M. SHELX86 and SHELXL93, University of Göttingen

(29) Hoffmann, R. *J. Chem. Phys.* **1963**, *39*, 1397.

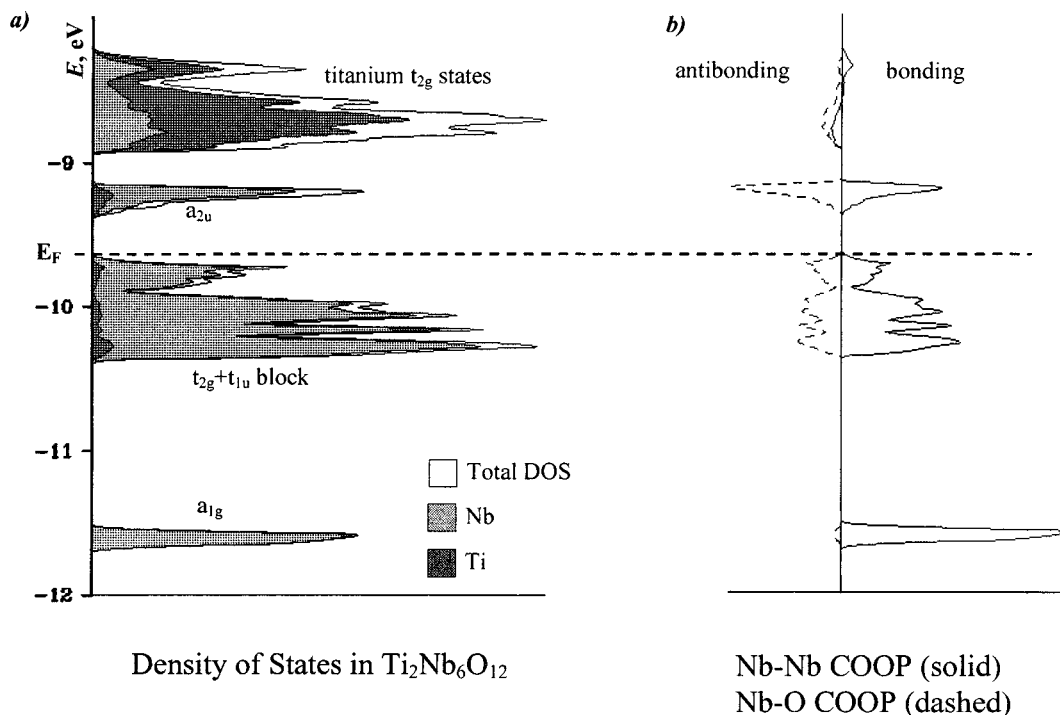


Figure 5. Total density of states (DOS) and Nb and Ti contributions to the DOS around the Fermi level (a) and intracluster Nb–Nb and Nb–O COOP curves for $\text{Ti}_2\text{Nb}_6\text{O}_{12}$ (b).

were calculated by using a set of 12 k-points uniformly distributed over the asymmetric unit of the Brillouin zone, and a set of 88 k-points was used to verify the convergence. For the band dispersion curves calculations, the k-point sets used contained 30 points per line.

Magnetic Measurements. The magnetic susceptibility of a $\text{Ti}_2\text{-Nb}_6\text{O}_{12}$ powder sample was measured with a Quantum design SQUID magnetometer at 4 T, in the temperature range of 2–300 K. The data were corrected for the contribution of 2 mass % NbO impurity. The magnetic susceptibility of the NbO powder used in the synthesis of $\text{Ti}_2\text{Nb}_6\text{O}_{12}$ was measured and used to account for the correction. The measured susceptibility of NbO was found to be within the range of the previously reported data.³²

Resistivity Measurements. The electrical resistivity was measured in the temperature range 10–300 K by using the four-probe technique on a powder sample of $\text{Ti}_2\text{Nb}_6\text{O}_{12}$ pressed into a pellet of $0.07 \times 2.00 \times 3.70 \text{ mm}^3$.

Results

Crystal Structure Description. $\text{Ti}_2\text{Nb}_6\text{O}_{12}$ crystallizes in an original structure type (Figure 2), with one formula unit in the primitive rhombohedral unit cell (space group $R\bar{3}$).

The main building block of this structure is an octahedral $(\text{Nb}_6\text{O}_{12})\text{O}_6^a$ cluster unit. The cluster has crystallographically imposed S_6 symmetry, and the Nb_6 octahedron is slightly compressed along the 3-fold axis ($\text{Nb-Nb}_{(\Delta)} = 2.8502(4) \text{ \AA}$, $\text{Nb-Nb}_{(\Delta-\Delta)} = 2.7896(4) \text{ \AA}$). The average Nb–Nb distance (2.8199 \AA) is typical for niobium oxides containing octahedral clusters.⁹ The Nb–O distances also correspond to the typical values for these systems ($\text{Nb-O}^a = 2.212(2) \text{ \AA}$, $\text{Nb-O}_{\text{ave}}^i = 2.096 \text{ \AA}$). The clusters connect to each other via “outer–inner”

linkages to form a three-dimensional network (Figure 1a). Every cluster unit shares all its outer and six inner oxygens with six neighboring clusters, thus the framework connectivity formula can be written as $(\text{Nb}_6\text{O}_{6/2}^{i-a}\text{O}_6^i)\text{O}_{6/2}^{a-i}$. Every two clusters are connected by two niobium–oxygen bonds resulting in a relatively short Nb–Nb intercluster distance (3.3156(5) \AA).

The titanium atoms in $\text{Ti}_2\text{Nb}_6\text{O}_{12}$ are located on a 3-fold axis above and below each cluster, and have a distorted octahedral environment (Figure 3a). The TiO_6 octahedron is formed by three “inner” oxide ligands belonging to three clusters, and three “outer–inner” oxide ligands belonging to another cluster (Figure 3b). The shortest Nb–Ti distance is 3.1757(3) \AA .

The crystal structure of $\text{Ti}_2\text{Nb}_6\text{O}_{12}$ is characterized by the presence of large cubeoctahedral cavities formed by 6 “inner” and 6 “outer–inner” oxide ions. The centers of these cavities lie on the 3-fold axes, between the titanium ions (Figure 2). The distance from the center of the cavity to the nearest oxygen ligand is 2.92 \AA .

Magnetic Properties. The molar magnetic susceptibility of $\text{Ti}_2\text{Nb}_6\text{O}_{12}$ as a function of temperature is shown in Figure 4. The compound exhibits temperature-independent paramagnetism between 100 and 300 K, with $\chi_{290} = 3.7 \times 10^{-4} \text{ emu/mol}$. An increase of magnetic susceptibility below 100 K results from Curie–Weiss contribution with an effective magnetic moment corresponding to ca. 0.18 unpaired electrons per formula unit. This value is probably caused by other impurities rather than by the presence of localized unpaired electrons in the bulk material.

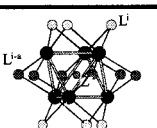
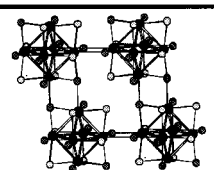
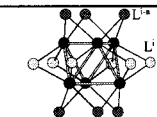
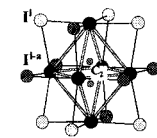
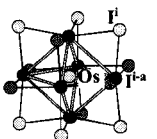
Electrical Resistivity Properties. The electrical resistivity of $\text{Ti}_2\text{Nb}_6\text{O}_{12}$ increases exponentially with decreasing temperature, indicating a semiconducting behavior. The resistivity at room temperature is approximately $2 \text{ } \Omega\cdot\text{cm}$. The thermal activation energy for conduction, estimated from the linear portion of the plot of $\ln \rho$ vs $1/T$ in the temperature range 100–300 K, is 0.052 eV.

(30) Hoffmann, R. *Solids and Surfaces: A Chemist's View of Bonding in Extended Structures*; VCH Publishers: New York, 1988, and references therein.

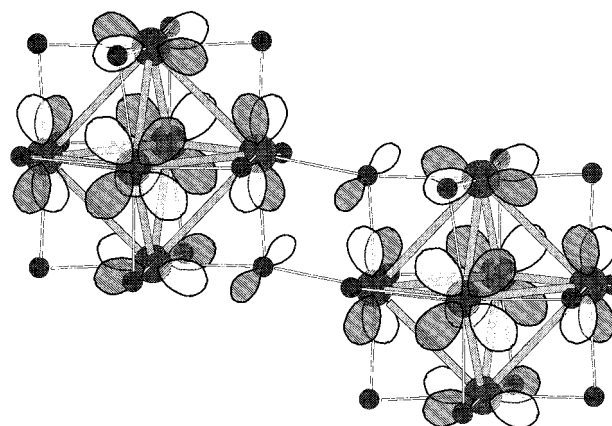
(31) Whangbo, M.-H.; Evain, M.; Hughbanks, T.; Kertesz, M.; Wijeyesekera, S.; Wilker, C.; Zheng, C.; Hoffmann, R. *Extended-Hückel Molecular, Crystal, and Properties Package*; Quantum Chemical Program Exchange, 1989.

(32) (a) Khan, H. R.; Raub, C. J.; Gardner, W. E.; Fertig, W. A.; Johnson, D. C.; Maple, M. B. *Mater. Res. Bull.* **1974**, *9*, 1129–1136. (b) Brauer, G. *Z. Anorg. Chem.* **1948**, *256*, 10–14.

Table 5. Comparison between Cluster Frameworks of the Compounds A_nM₆L₁₂(Z)

	Basic Cluster Unit ^a	Cluster Linkage
Zr ₆ L ₁₂ (Z) ¹⁹ and MM ₆ L ₁₂ (Z) ²⁰⁻²³		
Ti ₂ Nb ₆ O ₁₂ and CsEr ₆ I ₁₂ (C) ²⁴		same linkage pattern in (ab), (bc) and (ac) planes
Cs ₂ Pr ₆ I ₁₂ (C ₂) ²⁵		linkage pattern in (ab) plane linkage pattern in (bc) and (ac) planes
K ₂ La ₆ I ₁₂ (Os) ²⁶		linkage pattern in (ac) plane linkage pattern in (bc) plane linkage pattern in (ab) plane

Band Structure Description. The density of states (DOS) curve in the energy region near the Fermi level is shown in Figure 5a. The bands at about -11.6, -10, and -9.2 eV correspond to niobium–niobium bonding states. The band at -9.2 eV is not occupied because for this band, in contrast to the lower Nb-based states, the antibonding niobium–oxygen

**Figure 6.** Schematic representation of orbital contributions to the “a_{2u}” band at the Γ point. No significant interactions between the clusters are expected due to the δ symmetry of niobium orbitals with respect to the outer ligands.

interactions present in all these states dominate over niobium–niobium bonding contribution (Figure 5b). The position of the Fermi level corresponds to 14 valence electrons per cluster. Titanium d states are located higher in energy and are empty, which indicates that titanium is present in the +4 oxidation state. This result is also supported by bond valence sum calculations³³ that give a bond order of 3.85 for titanium. The band structure calculation suggests that the title compound is expected to be an indirect gap semiconductor with a gap of about 0.3 eV, which is quite consistent with the experimental results.

The overlap populations corresponding to Nb–Ti and Nb–Nb intercluster interactions are 0.037 and -0.008, respectively, which can be neglected compared to the average Nb–Nb intracluster overlap population found to be 0.278.

An important feature of the band structure of the title compound is the narrowness of the frontier band “a_{2u}” that originates from the “a_{2u}” molecular orbital of the cluster. It has δ -symmetry with respect to the outer ligands, which leads to the absence of significant interactions between the neighboring clusters (Figure 6), resulting in small dispersion of the band and high density of states. Band structure calculations on the cluster framework alone (excluding titanium atoms) result in a narrower “a_{2u}” band, indicating that the slight broadening of this band upon inclusion of titanium is caused by interactions between the titanium d states and the clusters.

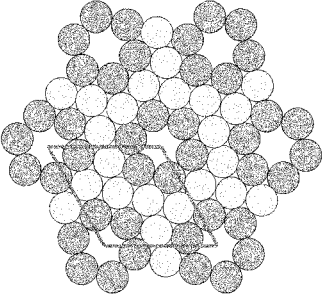
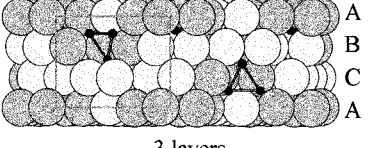
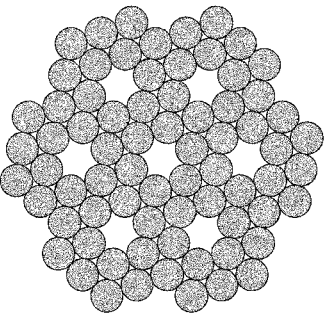
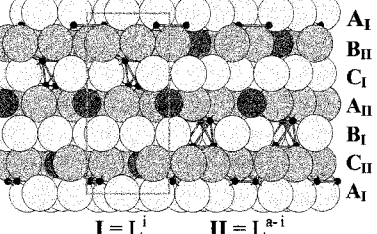
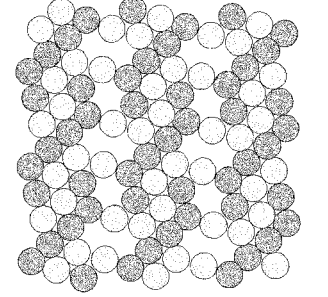
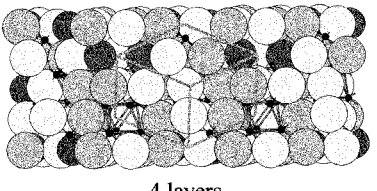
Discussion

Structural Relationships between Ti₂Nb₆O₁₂ and A_nM₆L₁₂(Z). These compounds are based on cluster frameworks in which the clusters are connected exclusively by “inner–outer” linkages in three dimensions. The structural relationships between Ti₂Nb₆O₁₂ and the A_nM₆L₁₂(Z) series which contain interstitially stabilized M₆L₁₈(Z) clusters are summarized in Tables 5 and 6. The majority of the A_nM₆L₁₂(Z) phases have structures that can be derived from the parent “Zr₆L₁₂” structure type originally reported by Corbett et al. in 1978.³⁴ This structure is based on a three-layer cubic close packing of anions in which each layer is formed by both “inner” and “inner–outer” ligands. One out of every 13 anionic sites within each layer is vacant and coincides with the cluster center. MM₆L₁₂(Z) phases,²⁰⁻²³ also based on this cluster framework, contain M³⁺ ions in the

(33) Brown, I. D.; Altermatt, D. *Acta Crystallogr. Sect. B* **1985**, *41*, 244–247.

(34) Corbett, J. D.; Daake, R. L.; Poeppelmeier, K. R.; Guthrie, D. H. J. *Am. Chem. Soc.* **1978**, *100*, 652–654.

Table 6. Relationship between the Structures of $A_nM_6L_{12}(Z)$ in Terms of Anionic Close Packing^a

	Ref	Basic anionic layer	Layer sequence	Cluster location	Cavities filling (per cluster)
$Zr_6L_{12}(Z)$	19			vacancies in all layers	6 square-pyramidal – Zr_6 1 cubeoctahedral (center of the cluster) – Z 7 octahedral – empty
$MM_6L_{12}(Z)$	20-23	1 vacancy per 12 anions	3 layers		6 square-pyramidal – M_6 1 cubeoctahedral (center of the cluster) – Z 1 octahedral – M^{3+} 6 octahedral – empty
$Ti_2Nb_6O_{12}$	this work			vacancies in type I layers only	6 square-pyramidal – Nb_6 1 cubeoctahedral (center of the cluster) – empty 1 cubeoctahedral – empty 2 octahedral – Ti^{4+} 6 square-pyramidal – empty
$CsEr_6I_{12}(C)$	24	2 vacancies per 12 anions	$I = L^I$ $II = L^{A^I}$ 6 layers		6 square-pyramidal – Er_6 1 cubeoctahedral (center of the cluster) – C 1 cubeoctahedral – Cs^+ 2 octahedral – empty 6 square-pyramidal – empty
$Cs_2Pr_6I_{12}(C_2)$	25			1/3 vacancies ("single ones") in all layers	6 square-pyramidal – Pr_6 1 cubeoctahedral (center of the cluster) – C_2 2 cubeoctahedral – Cs^+ 1 square planar – empty 6 square-pyramidal – empty 2 sea-saw shaped- empty
$K_2La_6I_{12}(Os)$	26	No extended close packing			6 square-pyramidal – La_6 1 cubeoctahedral (center of the cluster) – Os 2 large irregular, $CN=8 - K^+$ all others ($CN \leq 8$) – empty

^a Light gray spheres represent "inner" ligands, medium gray represent "outer-inner" ligands, and dark gray represent cesium ions or the centers of cubeoctahedral cavities.

octahedral site at the center of the rhombohedral unit cell. Large cations such as Cs^+ lead to a new structure type $CsEr_6I_{12}(C)$,²⁴ in which the cluster linkage pattern is the same, but different anion packing leads to one additional cubeoctahedral cavity per cluster. In contrast to $MM_6L_{12}(Z)$, the layer sequence in $CsEr_6I_{12}(C)$ can be written as $A_I B_{II} C_I A_{II} B_I C_{II} \dots$, where the subscript I refers to layers formed by "outer-inner" ligands and the subscript II refers to layers formed by "inner" ligands. One out of every seven anionic sites is vacant in each layer. The Er_6 clusters occupy only the vacancies in type I layers, while cesium ions occupy only the vacancies in type II layers. Despite the similarity in their cluster linkage patterns and symmetry, the cluster frameworks of $MM_6L_{12}(Z)$ and $CsEr_6I_{12}(C)$ cannot be transformed into each other without bond breaking due to the different arrangement of "inner" and "outer-inner" ligands in the basic cluster units of these compounds. Further addition of

cesium ions results in the formation of the $Cs_2Pr_6I_{12}(C_2)$ structure type,²⁵ which contains two additional cubeoctahedral cavities per cluster, occupied by the cesium ions. In this compound, the cluster linkage pattern is no longer isotropic. The clusters are connected in the (ab) plane to form a pseudosquare net, while the clusters linkage pattern in (bc) and (ac) planes is the same as that in the $MM_6L_{12}(Z)$ structure type. The pseudosquare cluster arrangement resembles that observed in the "Chevrel phases" and leads to the formation of channels along the $[001]$ direction where the cesium ions are located. In contrast, the cesium sites in $CsEr_6I_{12}(C)$ are shielded by anions and are not accessible. Recently, Uma and Corbett reported the structure of $K_2La_6I_{12}(Os)$,²⁶ which is significantly different from that of $Cs_2Pr_6I_{12}(C_2)$. The clusters in $K_2La_6I_{12}(Os)$ are connected to each other via one $La-I$ bond (in the (100) plane), while in all other structure types described here the clusters are connected via two

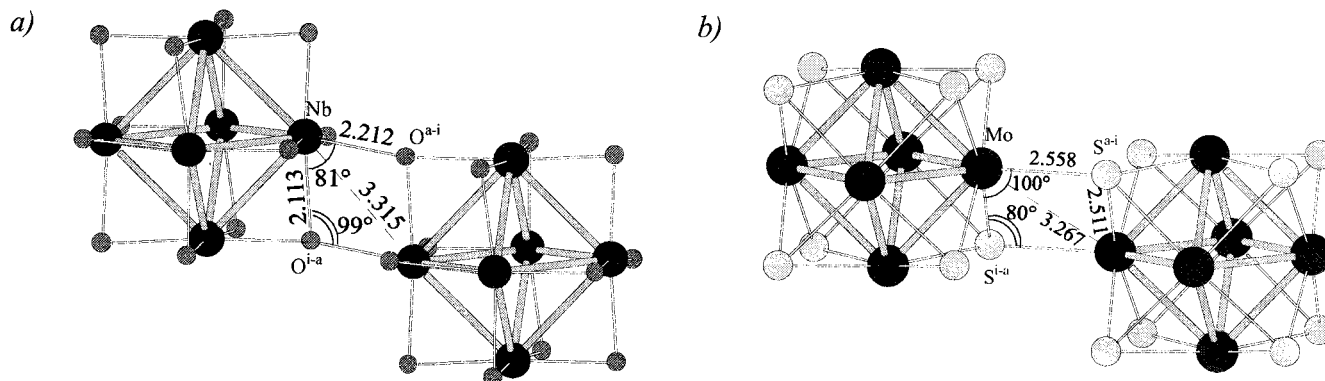


Figure 7. Bond distances and angles around intercluster linkages in Ti₂Nb₆O₁₂ (a) and in PbMo₆S₈ (b).

M–L bonds. In addition, the structure of K₂La₅I₁₂(Os) is not based on iodide close packing, presumably due to the size of the potassium ion, which is too small to occupy the cubeoctahedral cavity and too large to occupy the octahedral cavity.

The new niobium cluster oxide Ti₂Nb₆O₁₂ is based on a cluster framework similar to that found in CsEr₆I₁₂(C). However, these structure types differ in cation distribution. The framework of Ti₂Nb₆O₁₂ contains empty cubeoctahedral cavities similar to those occupied by Cs⁺ in CsEr₆I₁₂(C). Titanium ions in Ti₂Nb₆O₁₂ occupy octahedral cavities, which are empty in CsEr₆I₁₂(C). The stability of the CsEr₆I₁₂(C)-type framework in the case of Ti₂Nb₆O₁₂ is somewhat surprising because it does not contain a large cation that requires the presence of a cubeoctahedral cavity.

Similarities and Differences between Ti₂Nb₆O₁₂ and the “Chevrel Phases”. The key feature of the new niobium cluster oxide is its structural relationship to the “Chevrel phases”. The similarities can be seen in the connectivity patterns (Figure 1), and in the relationships between the average intra- and inter-cluster metal–metal distances. The respective distances are 2.8199 and 3.3154 Å in Ti₂Nb₆O₁₂ and 2.7021 and 3.2673 Å in PbMo₆S₈.³⁵ It is interesting to note that the intercluster Mo–Mo distance is smaller than the intercluster Nb–Nb distance, even though the Mo–S bond distance is larger than the Nb–O distance (Figure 7). This can be explained by the fact that in the Mo₆S₈ⁱS₆^a cluster, the molybdenum atoms are located slightly above the plane formed by “inner” sulfur atoms, and the S^{i-a}–Mo–S^{i-a} angles are greater than 90° allowing for closer contacts between molybdenum atoms.²⁷ In the case of Ti₂Nb₆O₁₂, the O^{a-i}–Nb–O^{i-a} angle is smaller than the Nb–O^{i-a}–Nb angle, and ligand steric effects force the niobium atoms to be further apart.

In addition to their structural similarities, Ti₂Nb₆O₁₂ and the “Chevrel phases” show comparable features in their band structures. The highest occupied band in PbMo₆S₈ originates from the “e_g” MO of the Mo₆S₈ cluster unit, and has δ symmetry with respect to the outer ligands, similar to the “a_{2u}” orbital in the Nb₆O₁₂ cluster. Thus, when the Mo₆S₈ units are assembled in the extended structure, the “e_g” MO leads to a weakly dispersed band.³⁶ In PbMo₆S₈, this band is half filled resulting in a high density of states at the Fermi level, presumably one of the factors responsible for superconductivity in the “Chevrel phases”.¹⁴ One of the main results of our calculations is the prognosis that populating the “a_{2u}” orbital in the Nb₆O₁₂ cluster in the Ti₂Nb₆O₁₂ structure type would lead to a compound whose

highest occupied band is similar to the highest occupied band in PbMo₆S₈. The 14-electron cluster configuration present in Ti₂Nb₆O₁₂ is the most stable cluster electronic configuration for niobium oxides containing octahedral clusters; however, compounds with 15 electrons per cluster, such as NaNb₁₀O₁₈³⁷ and LaNb₈O₁₄,³⁸ have been reported. We are currently investigating whether 15-electron compounds can be obtained in the Ti₂Nb₆O₁₂ structure type by insertion of monovalent cations in the cubeoctahedral cavities present in the cluster framework. Comparative analysis of A_nM₆L₁₂(Z) structures and investigation of the role of the cation in the stability of different frameworks can be advantageously used to design and prepare new open-framework niobium and/or molybdenum oxide cluster compounds which mimic the “Chevrel phases” in terms of inter-cluster bonding.

Conclusions. Ti₂Nb₆O₁₂ can be considered a structural analogue of the “Chevrel phases” in terms of intercluster connectivity and metal–metal distances. As the basic cluster unit is changed from M₆L₁₄ to M₆L₁₈, the highest metal–metal bonding states maintain δ symmetry with respect to the “outer” ligands, which leads to narrow bands in the electronic structure of these compounds. However, in the superconducting “Chevrel phases” this band is partially occupied, while in Ti₂Nb₆O₁₂ it is the lowest unoccupied band. Similarities between frontier bands can lead to interesting physical properties of the title compound, if a one-electron reduction can be achieved. The presence of empty crystallographic sites in the structure and the small band gap indicate that the reduction could be achieved through insertion of monovalent cations.

Acknowledgment. We wish to thank Dr. Hanno zur Loye, University of South Carolina, for the magnetic measurements; Dr. James Eckert, Yale University, for EDS and WDS analyses; and Dr. Shiou-Jyh Hwu, University of South Carolina, for conductivity measurements. This research was supported in part by Wake Forest University through the Research and Creative Activities Fund.

Supporting Information Available: Tables giving the details of data collection and refinement and anisotropic displacement parameters for Ti₂Nb₆O₁₂, band structure plot, and details of EDS and WDS analyses and conductivity measurements (PDF). This material is available free of charge via the Internet at <http://pubs.acs.org>.

(35) GuilleVIC, J.; Lestrat, H.; Grandjean, D. *Acta Crystallogr. Sect. B* **1976**, *32*, 1342–1345.

(36) Nohl, H.; Klöse, W.; Andersen, O. K. In *Superconductivity in Ternary Compounds*; Top. Curr. Phys. 32; Fischer, Ø., Maple M. B., Eds.; Springer-Verlag: Berlin, 1982.

JA990759E

(37) Köhler, J.; Simon, A. *Z. Allg. Anorg. Chem.* **1989**, *572*, 7–17.
(38) Köhler, J.; Tischtan, R.; Simon, A. *J. Chem. Soc., Dalton Trans.* **1991**, 829–832.